THIS MONTH IN

JNM

"Amphibian cars" for molecular imaging: Boerman and Oyen look at the challenges surrounding development of hybrid PET/MRI scanners and previews an article in this issue of *JNM* introducing a molecular probe that provides a signal in both modalities. . . ***Page 1213***

Single-session PET/CT staging mammography: Heusner and colleagues compare the diagnostic accuracy of an all-in-one protocol of whole-body ^{18}F-FDG PET/CT and integrated ^{18}F-FDG PET/CT mammography with that of a multimodality algorithm for initial breast cancer staging. . . . . ***Page 1215***

Breath-hold PET/CT in lung cancer: Kawano and colleagues describe the advantages of breath-hold over free-breathing PET/CT in providing more precise measurement of maximum SUVs. . . . ***Page 1223***

Optimal imaging for paraganglioma: Koopmans and colleagues evaluate the diagnostic accuracies of ^{111}In-octreotide somatostatin receptor scintigraphy, ^{123}I-MIBG scintigraphy, and morphologic imaging in patients with highly suspected head and neck paragangliomas. . . . . ***Page 1232***

Gene modulation of ^{18}F-FDG kinetics: Strauss and colleagues use PET imaging and histopathologic results to assess the effects of angiogenesis-related gene expression on ^{18}F-FDG kinetics in patients with primary colorectal tumors. . . . . ***Page 1238***

^{11}C-choline PET in hepatocellular cancer: Yamamoto and colleagues explore the potential utility of ^{11}C-choline PET as a complement to ^{18}F-FDG PET in the detection of hepatocellular carcinoma lesions. . . . . ***Page 1245***

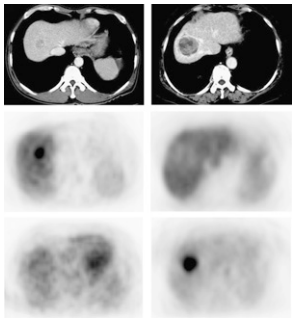

^{11}C-(*R*)-PK11195 imaging in AD: Tomasi and colleagues report on a reference region model for estimating the binding potential of a PET radiotracer that shows increased microglial activity and decreased vascular binding in individuals with Alzheimer's disease. . . . . ***Page 1249***

Opioidergic system and rewards: Schreckenberger and colleagues use ^{18}F-DPN to investigate the neurobiologic correlates of reward dependence and discuss the implications of these findings for predicting predisposition to addictive behavior. . . ***Page 1257***

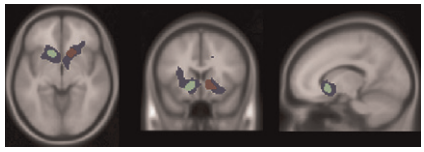

Voxel-based diagnosis of Alzheimer's disease: Mikhno and colleagues explore the utility of ^{11}C-PIB PET imaging of amyloid-β accumulation in discriminating healthy individuals from those with Alzheimer's disease. . . . . ***Page 1262***

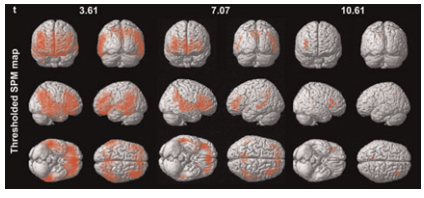

Novel transporter radioligand: Arakawa and colleagues report on several methods for quantification of (S,S)-^{18}F-FMeNER-D_2, a PET imaging agent with promise for direct estimation of norepinephrine transporter occupancy by antidepressants. . . . . ***Page 1270***

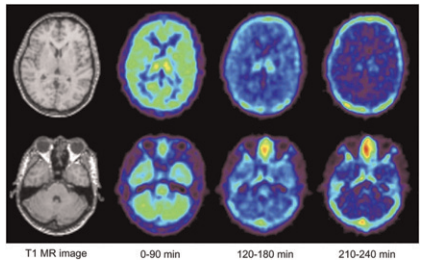

Reversal of vascular ^{18}F-FDG uptake: Lee and colleagues evaluate serial changes in vascular ^{18}F-FDG uptake in response to lifestyle interventions and discuss the potential use of this technique in atherogenic risk reduction. . . . . ***Page 1277***

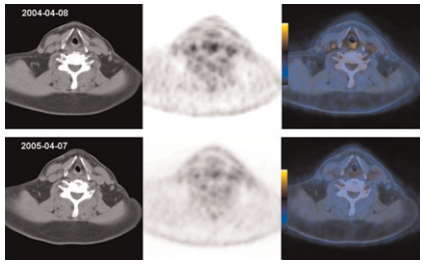

Gated SPECT in atrial fibrillation: Sciagrà and colleagues examine differences in myocardial perfusion between simultaneously acquired gated and nongated SPECT data in patients with atrial fibrillation and provide recommendations for optimal assessment. . . . . ***Page 1283***

Viability in ventricular aneurysms: Zhang and colleagues describe long-term benefits of SPECT and PET in assessing the viability of aneurysmal myocardium in patients with ischemic cardiomyopathy and compare short-term results in those undergoing revascularization or revascularization plus aneurysmectomy. . . . . ***Page 1288***

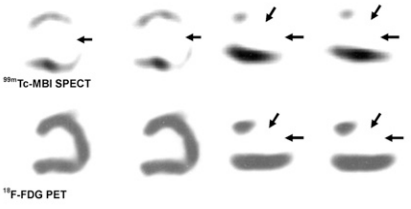

Human biodistribution of ^{99m}Tc-N-DBODC: Cittanti and colleagues assess the safety profile and biodistribution of a new myocardial perfusion tracer that promises to provide early and high-quality SPECT images of the left ventricle. . . . . ***Page 1299***

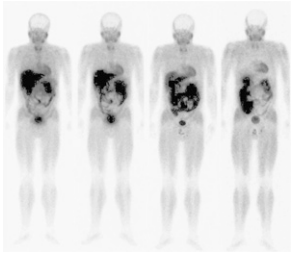

Overview of SPECT/CT: Buck and colleagues offer an educational review of the current status and future prospects of hybrid SPECT/CT in cardiac, neurologic, and oncologic applications. . . ***Page 1305***

Diabetes and myocardial glucose use: Shoghi and colleagues investigate myocardial glucose metabolism in a rodent model of type 2 diabetes and validate PET measurements of glucose uptake against gene and protein expression of glucose transporters. . . . . ***Page 1320***

Functional P-gp activity at the BBB: Bankstahl and colleagues use (*R*)-^{11}C-verapamil PET and tariquidar, a new-generation P-glucoprotein modulator, to study functional activity at the blood–brain barrier in rats. . . . . ***Page 1328***

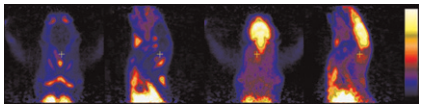

Pharmacokinetics of ^{99m}Tc(N)-DBODC(5): Bolzati and colleagues elucidate the mechanisms of distribution, retention, and elimination of a promising myocardial imaging agent and describe the potential for extension to tumor imaging and noninvasive multidrug resistance studies. . . . . ***Page 1336***

Imaging PtdE availability: Zhao and colleagues report on the development of ^{99m}Tc-duramycin as a novel molecular probe for imaging phosphatidylethanolamine, a major phospholipid externalized to the surface of apoptotic cells and accessible in necrotic cells. . . . . ***Page 1345***

Cytotoxicity of ^{111}In-DTPA-hEGF: Cai and colleagues investigate the relationships among human epidermal growth factor expression, DNA damage, and cytotoxicity in cells exposed to an Auger electron–emitting radiopharmaceutical. . . . ***Page 1353***

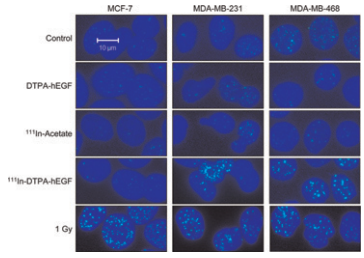

PET/MRI in pancreatic cancer: von Forstner and colleagues compare uptake of ^{18}F-FDG, ^{18}F-FLT, and ^{18}F-FEC in human pancreatic tumor cell lines in mice and correlate tumor uptake with gene expression of membrane transporters and rate-limiting enzymes. . . . . ***Page 1362***

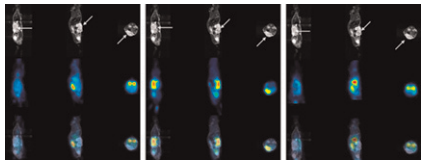

Bifunctional PET/MRI probe: Lee and colleagues detail the development of a bifunctional iron oxide nanoparticle probe for PET and MRI scans of tumor integrin $\alpha_v\beta_3$ expression. . . . . ***Page 1371***

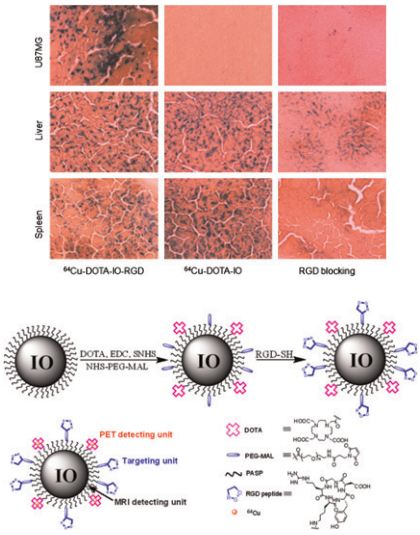

^{99m}Tc-HMPAO in RA: Bennink and colleagues assess the biodistribution and radiation dosimetry of ^{99m}Tc-HMPAO–labeled monocytes in adult patients with rheumatoid arthritis and describe the potential applications in noninvasive monitoring of therapy and disease progression. . . . . ***Page 1380***

^{18}F-FDG in colorectal tumor cells: Sharma and Smith look at therapy-induced changes in tracer incorporation at the tumor cell level in response to conventional and novel chemotherapy agents. . . . . ***Page 1386***

Case against radioiodine ablation: Hay and colleagues take issue with widely used postoperative radioiodine remnant ablation as adjuvant therapy in patients with well-differentiated thyroid carcinoma and outline reasons for suggesting that ablation is often the wrong choice. . . . ***Page 1395***

ON THE COVER

The maximum SUV of free-breathing PET should not be accepted as accurate, especially in the lower lung and for small pulmonary lesions. In this patient, blurring of ^{18}F-FDG accumulation was more apparent in fusion free-breathing PET/CT (top) than in fusion breath-hold PET/CT (bottom). Breath-hold imaging realizes a complete match between CT and PET and is thus recommended as part of the standard protocol for lung cancer.

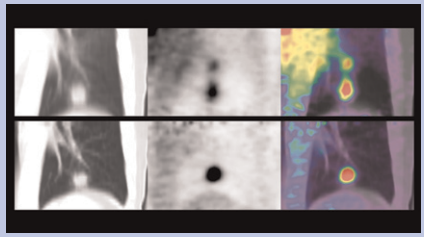

See page 1229.